MgB_2 radio-frequency superconducting quantum interference device prepared by atomic force microscope lithography

M. Gregor, T. Plecenik, M. Praščák, R. Mičunek, M. Kubinec, V. Gašparík, M. Grajcar, P. Kúš and A. Plecenik.
Department of Experimental Physics,Comenius University, SK-84248 Bratislava, Slovakia
(Dated: February 1, 2008)

A new method of preparation of radio-frequency superconducting quantum interference devices on MgB_2 thin films is presented. The variable-thickness bridge was prepared by a combination of optical lithography and of the scratching by an atomic force microscope. The critical current of the nanobridge was 0.35 μA at 4.2 K. Non-contact measurements of the current-phase characteristics and of the critical current vs. temperature have been investigated on our structures.

Since the discovery of superconductivity in of MgB_2,[1] many techniques have been used to prepare superconducting weak links, the basic element of superconducting devices. The relatively high critical temperature of MgB_2, its metallic character, good stability and low anisotropy could guarantee superior properties of MgB_2 weak links and superconducting quantum interference devices (SQUID). Weak links with non-tunnel-type conductivity have been attracting increasing attention, such as point contact, Dayem type bridge, constant and variable thickness bridge. The main advantage of non-tunnel-type junctions is their low capacitance. Nanobridges, with dimensions L_{eff} sufficiently small relative to the superconducting coherence length ξ, have nearly ideal Josephson behavior. The reported value of the coherence length in MgB_2 is 5.2 nm.[2] Importantly, also a wider bridge can show Josephson current-phase relationship, provided that the width of the bridge is comparable to, or smaller then the effective London penetration depth λ_{eff}. Reported values for the MgB_2 bulk penetration depth λ vary from 140 to 180 nm.[3] Zhang et al.[4] reported an MgB_2 point contact SQUID working at 19 K. Burnell et al.[5] realized an MgB_2 thin film SQUID by localized ion damage, operated up to 20 K. Several groups prepared SQUIDs using the focused ion beam and produced nanobridges with dimensions smaller than the effective London penetration depth λ_{eff}.[3] Burnell et al.[6] reported an MgB_2 SQUID prepared by FIB operated from 10 K to 24 K, with magnetic flux noise at 20 K as low as 14 $\mu\Phi_0/\sqrt{\text{Hz}}$. Atomic Force Microscope (AFM) lithography has become a powerful technology, which allows to create structures with a nanometer scale resolution suitable for cryogenic application. Atomic force microscope can pattern surface in different ways - by local oxidation or by scratching. Some researchers published technology of local electrochemical oxidation of the surface of Nb and NbN thin films by voltage biased tip[7] and produced Dayem and variable thickness nanobridges. Others produced nanostructures using tip-surface mechanical interaction leading to surface plowing or scratching[8] and produced a typical a Dayem-type bridge in an Al film with dimensions 100×100 nm^2. We focus our attention on the preparation of an RF-SQUID variable-thickness bridge in the MgB_2 superconductor by AFM scratching through the photoresist. The main advantage of our approach is the possibility to prepare nanostructures on the hard materials through the resist without ion damage, which is produced in focused ion beam etching. By post-etching with low energy Ar ions we are able to continuously change the dimensions of the bridge.

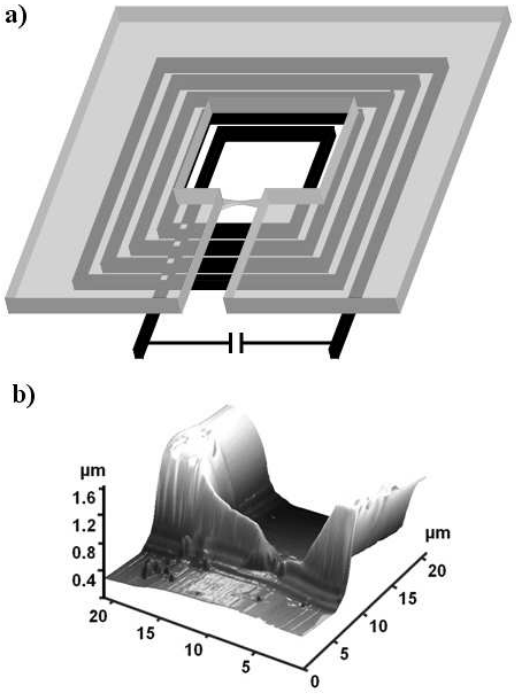

FIG. 1: a) A design of the SQUID. b) AFM scan of the MgB_2 variable thickness bridge prepared on a 200 nm MgB_2 thin film with a 1.5 μm thick photoresist

Superconducting MgB_2 thin films were prepared by magnetron sputtering on the sapphire substrate and ex-situ annealing in a vacuum chamber. The deposition process was realized by two independent magnetrons. The technology of MgB_2 thin film preparation was described in Ref. 9. Atomic Force Microscope has been used for surface roughness analysis of thin films as well as for preparation of the weak links. RMS (Root Mean Square) roughness of the MgB_2 thin films was below 10 nm.[10] The surface scanning has been done in the semi-contact mode using standard Si tip with W_2C coating or

diamond like coating. The maximum lateral scan range of the piezo tube is 50×50 μm^2, the maximum vertical range is 2 μm. Typical curvature radius of the tip is 30 nm and the resonant frequency is about 255 kHz. The spring constant of the cantilevers was 20-30 N/m. An RF-SQUID with microstrip (see Fig. 1a) was formed by optical lithography (3 μm wide strip) on the smooth MgB_2 thin films. The critical temperature of a 3-μm strip was 31.3 K. Our SQUID consists of a washer (50×50 μm inner and 2000×2000 μm outer dimension) for better concentration of the magnetic flux and of a 10 μm wide slit. We used a positive photoresist for direct optical lithography and argon ion etching with energy of the ions 650 eV and ion current 50 mA for determination of the microstructure. After formation of the structures by Ar ion etching, the resist was not removed from the MgB_2 strip, but AFM scratching was applied to the micro-strip with 10 μm length and 3 μm width in order to form the variable-thickness bridge. The AFM scratching (nanolithography) was done by increasing the deflection of the cantilever in the contact mode. The width and the depth of the grooves depend on the deflection force. Because the photoresist is a very soft material it was hard to determine the sizes of the grooves and the applied force. We repeatedly scratched through the same place until the photoresist was removed. By scratching the resist across the strips we produced a small variable-thickness bridge with submicrometer dimensions. We applied additional Ar ion beam etching and gradually removed MgB_2 from the strip, so that we achieved the final thickness and width of the MgB_2 strip a few nm and about 100 nm, respectively. Figure 1b) shows the variable-thickness bridge before removing the photoresist (thickness of the MgB_2 film was 200 nm and thickness of the photoresist was 1.4 μm). The investigated SQUID was placed close to a parallel LC tank circuit. This resonant detection system consists of a solenoid copper coil ($L_T \approx 73$ nH) and a small capacitance ($C_T \approx 700$ pF). The tank circuit is fed from a current source at the resonant frequency 24 MHz, which produces alternating flux in the SQUID of amplitude $MQI_b \sin \omega_0 t$, where $Q = 80$ is the quality factor of our tank circuit, $M \approx 0.12$ nH is the mutual inductance and $I_b \sin \omega_0 t$ is the bias current. The DC flux in the SQUID is produced by the same copper coil. The signal from the tank circuit is amplified by the first stage of a cold amplifier located close to the tank circuit at liquid helium temperature. The cryogenic amplifier consists of a high electron mobility field effect transistor promoting low noise figure (0.4dB), high gain (18dB), and wide dynamic range. This amplifier stage provides the impedance matching to the 50 Ω coaxial cable and approximately 10dB gain. The output signal is further amplified by the next stages at room temperature. The second stage is of a similar design as the cryogenic stage and the last stage is a 30dB (Monolithic Microware Integrated Circuit) gain block. The overall gain is above 50dB with noise figure about 0.5dB at room temperature. The amplified signal is fed to a phase sensitive detector (Lock-in amplifier) from which the output is the amplitude and phase of the signal relating to the reference signal from the RF generator. Data acquisition and the measurement process is computer controlled via GPIB interface.

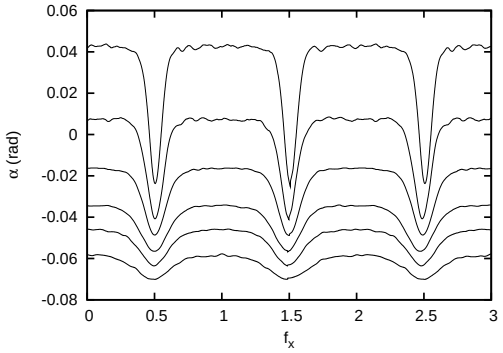

FIG. 2: Phase shift between the voltage across the tank and the driving current measured at various temperatures as a function of the normalized external magnetic flux $f_x = \Phi_x/\Phi_0$. From top to bottom, the data correspond to T=4.2, 6.4, 7.8, 9, 10.4, and 12.6 K.

The SQUID phase characteristics $\alpha(f_x)$, where α is the phase shift between the bias current I_b and the voltage across the tank circuit, and $f_x = \Phi_e/\Phi_0$ is external magnetic flux Φ_e normalized to the magnetic flux quantum Φ_0, are shown in Fig.2. In order to obtain more information on the microbridge superconducting weak link, we have calculated its current-phase relationship (CPR) $I_s(\varphi) = I_c f(\varphi)$ using the modified Rifkin-Deaver method[11,12]. The resonance frequency of the tank circuit depends on the effective inductance defined as[13,14]

$$L_{eff}(\varphi) = L\left(1 + \frac{1}{\beta f'(\varphi)}\right) , \qquad (1)$$

where L is the inductance of the washer, $\varphi = 2\pi\Phi/\Phi_0$ is the gauge-invariant phase difference across the Josephson

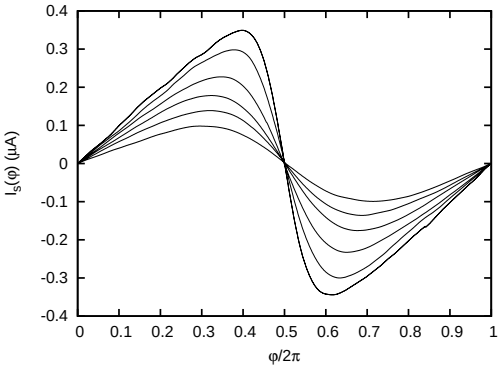

FIG. 3: $I_s(\varphi)$ characteristics calculated from the phase characteristics (see Fig. 2). The curves corresponds to temperature, from top to bottom, T=4.2, 6.4, 7.8, 9, 10.4, and 12.6 K.

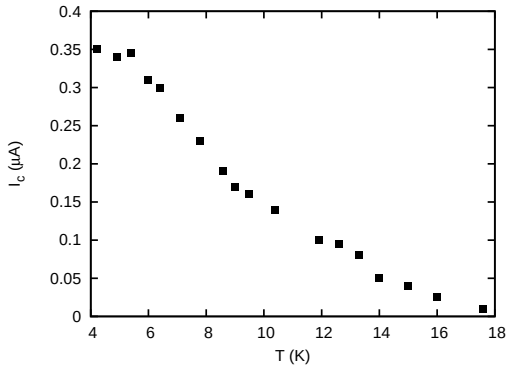

FIG. 4: Temperature dependence of the critical current of the weak link.

junction, Φ is the internal flux in the washer, Φ_0 is the elementary magnetic flux quantum and $\beta = 2\pi LI_c/\Phi_0$ is the normalized SQUID inductance. If $\beta < 1$, *i.e.* if the SQUID is in a nonhysteretic mode, we can determine the current-phase relationship from the relation[12]

$$I_s(\varphi) = \frac{L_T(\Delta I)^2}{2\pi Q\Phi_0}\int_0^{\varphi}\tan\alpha(\phi)d\phi \ , \qquad (2)$$

where L_T is inductance of the tank coil, $\Delta I = 16.5\ \mu A$ is the magnitude of the current in the coil producing magnetic flux Φ_0 in the rf squid, Q is the quality factor of the tank circuit and $\phi = 2\pi\Phi_e/\Phi_0$ is the normalized external *dc* magnetic flux. The phase shift $\alpha(\phi)$ between the voltage across the tank and the driving current is measured experimentally. The calculated current-phase characteristics are shown in Fig. 3. The maximum of the $I_s(\varphi)$ characteristics is shifted towards $\varphi = \pi$. Such deviation from standard Josephson sinusoidal behavior was predicted by Kulik and Omelyanchuk[15,16] for short Josephson junctions $d_{eff} \ll \xi$, where d_{eff} is the effective length of the weak link.[17] However, this condition can be hardly satisfied since $\xi \approx 5$ nm. Thus, we believe that the weak links are in the dirty limit and the shift of the maximum of the $I_s(\varphi)$ characteristics is caused by the enhanced kinetic inductance of the junction. The kinetic inductance can be characterized by the parameter[17]

$$l = 2\pi\frac{\mathcal{L}I_c}{\Phi_0} \ , \qquad (3)$$

where $\mathcal{L}$ is the kinetic inductance of the weak links. If l is larger than unity the $I_s(\varphi)$ becomes multivalued and the SQUID is in a hysteretic regime even for $\beta < 1$. This parameter is important since the large value of l deteriorates parameters of the superconducting weak links, especially the SQUID performance.[17] However, our SQUID is in the nonhysteretic regime, i.e. with $l < 1$ as one can expect for variable-thickness bridges.[17,18] The thickness, width and length of the bridge in the thinnest region is estimated from the AFM picture (Fig. 1b) to be 10, 200, and 100 nm, respectively.

Also the temperature dependence (compare Fig. 4 with Fig. 9 in Ref. 17 or Fig. 14 in Ref. 12) indicates that the weak link is long with $d_{eff} > \xi$ and that the critical temperature of the bridge T_c' is suppressed ($T_c' < T_c$). Similar temperature dependences were measured also by other groups. For example, AFM (Fig. 4), focused-ion-beam patterned nanobridges[3], as well as MgB_2 break junctions[19] have similar behavior of the critical current as a function of temperature with critical temperature, $T_c \approx 20$ K. It is striking that different technologies of weak link preparation give nearly identical results.

To conclude, our results show that AFM scratching through a soft material (in our case the photoresist) is a powerful technology which can produce MgB_2 weak links with a single valued Josephson current-phase relationship ($l < 1$). Even if etching was performed step-by-step without the contact for checking the etching speed, reproducibility of this process was 80%. Such weak links are promising for practical application and they can be incorporated into Josephson effect devices.[17,20]

Acknowledgments

This work was supported by grant VEGA 1/2011/05, APVT projects No. APVT-51-016604, APVT-20-011804 and project aAV/1126/2004.

Refferences

[1] J. Nagamatsu, N. Nakagawa, T. Muranaka, Y. Zenitani, and J. Akimitsu, Nature **410**, 63 (2001).
[2] D. K. Finnemore, J. E. Ostenson, S. L. Bud'ko, G. Lapertot, and P. C. Canfield, Phys. Rev. Lett. **86**, 2420 (2001).
[3] A. Brinkman, D. Veldhuis, D. Mijatovic, G. Rijnders, D. H. A. Blank, H. Hilgenkamp, and H. Rogalla, Appl. Phys. Lett. **79**, 2420 (2001).
[4] Y. Zhang, D. Kinion, J. Chen, J. Clarke, D. G. Hinks, and G. W. Crabtree, Appl. Phys. Lett. **79**, 3995 (2001).
[5] G. Burnell, D.-J. Kang, H. N. Lee, S. H. Moon, B. Oh, and M. G. Blamire, Appl. Phys. Lett. **79**, 3464 (2001).
[6] G. Burnell, D. J. Kang, D. A. Ansell, H. N. Lee, S. H. Moon, E. J. Tarte, and M. G. Blamire, Appl. Phys. Lett. **81**, 102 (2002).
[7] M. Fraucher, T. Fournier, B. Pannetier, C. Thirion, W. Wernsdorfer, J. Villegier, and V. Bouchiat, Physica C **368**, 211 (2002).
[8] B. Irmer, R. H. Blick, F. Simmel, W. Gdel, H. Lorenz, and

J. P. Kotthaus, Appl. Phys. Lett. **73**, 2051 (1998).
[9] R. Mičunek, A. Plecenik, P. Kúš, M. Zahoran, M. Tomášek, M. v. T. Plecenik, M. Gregor, V. Jacko, M. K. J. Greguš, B. Grančič, and M. Mahel', Physica C **435**, 78 (2006).
[10] M. Gregor, R. Mičunek, T. Plecenik, T. Roch, A. Lugstein, E. Bertagnolli, I. Vávra, M. Štefečka, M. Kubinec, M. Leporis, V. Gašparík, P. Kúš, and A. Plecenik, arXiv:0705.4229v1, (2007).
[11] R. Rifkin and B. Deaver, Phys. Rev. B **13**, 3894 (1976).
[12] A. A. Golubov, M. Y. Kupriyanov, and E. Il'ichev, Rev. Mod. Phys. **76**, 411 (2004).
[13] A. H. Silver and J. E. Zimmerman, Phys. Rev. **157**, 317 (1967).
[14] A. Barone and G. Paterno, *Physics and Aplications of the Josephson Effect* (JOHN WILEY & SONS, New York, 1982).
[15] I. O. Kulik and A. N. Omelyanchuk, JETP Lett. **21**, 96 (1975).
[16] I. O. Kulik and A. N. Omelyanchuk, Soc. J. Low. Temp. Phys. **3**, 945 (1977).
[17] K. K. Likharev, Rev. Mod. Phys. **51**, 101 (1979).
[18] L. D. Jackel, W. H. Henkels, J. M. Warlaumont, and R. A. Buhrman, Appl. Phys. Lett. **29**, 214 (1976).
[19] R. S. Gonnelli, A. Calzolari, D. Daghero, G. A. Ummarino, V. A. Stepanov, G. Giunchi, S. Ceresara, and G. Ripamonti, Phys. Rev. Lett. **97**, 097001 (2001).
[20] K. Likharev, *Dynamics of Josephson Junctions and Circuits* (Gordon and Breach Science Publishers, Paris, 1984).